



Impact of the Fiber Length Distribution on Porous Sponges Originating from Short Electrospun Fibers Made from Polymer Yarn

Xiaojian Liao, Pin Hu, Seema Agarwal, and Andreas Greiner*

Ultralight highly porous sponges made of short electrospun polymer fibers have gained significant attention for a variety of applications. According to the established procedures, short electrospun fibers are obtained by cutting or homogenization of electrospun fibers in suspension, which yield fibers with inhomogeneous fiber length. The role of the fiber length distribution and the fiber length in the mechanical compressibility of the sponges is unknown. Therefore, as a model study, sponges made from suspensions of short electrospun poly(acrylonitrile) (PAN) fibers with controlled fiber length distribution are investigated, and the role of the fiber length distribution in the compressibility of the sponges is analyzed quantitatively. These sponges are also compared to the ones prepared by established procedure as a benchmark. It is found that the compression stress and modulus of ultralight sponges with monodisperse short fibers are respectively 32% and 45% higher than that made with polydisperse short fibers. The study also shows that sponges made from longer fibers have higher modulus in comparison to the sponges made from shorter fibers.

Recently, the potential of electrospun fibers was reported for the fabrication of novel electrospun fibrous sponges by the use of short electrospun fibers.^[4,6,14,16] Owing to flexible fabrication conditions and diversified electrospun fibers, the sponges displayed tunable densities, multifunctionality, and applicability for various applications, for instance, reversible manual compression,^[16] hydrophilic or super hydrophobic,^[17,18] electrics,^[19,20] respirable open cells,^[21] or scaffolds for tissue engineering.^[22,23] Thus, these sponges could perfectly overcome the mechanical brittleness of traditional inorganic aerogel and high cost of carbon aerogel problems, making them a perfect candidate for broad applications due to their high potential for functionalization.

So far, almost all the concepts to obtain ultralight sponges consist of fabrication of

short electrospun fiber suspensions by mechanical cutting and processing by self-assembly, followed by freeze-drying.^[10] Normally, the short fibers obtained by using mechanical cutting devices, such as homogenizer, mixer, blender, grinder, exhibit uncontrollable length and broad length distribution represented by the high coefficient of variation (CV),^[3,24–26] which is defined as the ratio of the standard deviation to the mean length. Simultaneously, beyond several different reported methods, such as chemical treatment,^[27] ultrasonication,^[28] electric spark,^[29] concentrated polymer brush,^[30] and direct electrospinning,^[31–33] the patterned UV-crosslinking^[34] and microcutting method^[35,36] based on highly aligned fibers enable the production of quasi-monodisperse short fibers. Short fiber dispersions with low CV have not been used to the best of our knowledge for the preparation of sponges. Consequently, the role of CV and fiber length in the morphology and mechanical properties of the sponges is unknown, which is, however, very important for basic understanding and numerous applications.

Herein, we present a new method for the preparation of short electrospun fiber dispersions with controlled CV and use them for the preparation of the sponges in order to evaluate the microstructure and mechanical properties. We show the cryo-microcutting of multifibrillar highly oriented electrospun poly(acrylonitrile) (PAN) yarns which resulted finally in short individual PAN fibers of well-controlled length. Fiber dispersions of different CVs were obtained by mixing of short fibers of different lengths, which were used for the preparation of sponges following the established method. We could clearly

1. Introduction

Ultralight porous 3D materials, with unique integral properties of ultralow density,^[1,2] low thermal conductivity,^[3–5] high porosity,^[6,7] and good mechanical properties,^[8,9] exhibit a large range of applications as absorption materials, in thermal insulation, electronic equipment, as scaffolds for tissue engineering, and stimuli-responsive materials.^[10–13] Traditional inorganic aerogels, however, normally suffer from mechanical brittleness originating from rigid intrinsic quality of inorganic materials, which restricts their applications.^[11,14] The carbon aerogels based on carbon nanotube and graphene were considered as the promising elastic porous 3D materials. Unfortunately, the high-cost precursors hinder their practical applications.^[11,15]

X. Liao, P. Hu, Prof. S. Agarwal, Prof. A. Greiner
Macromolecular Chemistry and Bavarian Polymer Institute
University of Bayreuth
95440 Bayreuth, Germany
E-mail: greiner@uni-bayreuth.de

The ORCID identification number(s) for the author(s) of this article can be found under <https://doi.org/10.1002/mame.201900629>.

© 2020 The Authors. Published by WILEY-VCH Verlag GmbH & Co. KGaA, Weinheim. This is an open access article under the terms of the Creative Commons Attribution License, which permits use, distribution and reproduction in any medium, provided the original work is properly cited.

DOI: 10.1002/mame.201900629



quantify the role of the fiber length distribution in the morphology and compression strength of sponges, which will be presented in detail in the following sections.

2. Experimental Section

2.1. Materials

PAN (M_n 120 000, co-polymer with 6 wt% methyl acrylate, Dolan), polyurethane (PU) synthesized in the authors' group according to the previous report (sample no. 8 in Lit.,^[37] M_n of 50 000), dimethylformamide (DMF; Fisher Chemical, 99.99%), dimethylsulfoxide (DMSO; Fisher Chemical, 99.99%), dioxane (technical grade), ethanol (technical grade), and acetone (technical grade) were used as received.

2.2. Fabrication of High Aligned Electrospun Fibrillar Yarn

The electrospun fibrillar yarns were fabricated following with some modifications a previously published procedure.^[38] The solution for electrospinning was prepared by dissolving about 1 g of PAN powder in a mixed solvent of 4.7 g of DMF and 0.97 g of acetone. As shown in the Figure 1, the angle (13 degrees of inclination), distance (40 cm) and altitude (perpendicular distance to the plane of the end of funnel: 2 cm) of two syringes were fixed in the homemade syringe holder set-ups. The feed rate of solution was about 0.5 mL h⁻¹. The two needle tips of syringe were connected separately to the positive and negative electrodes of DC power supplies, respectively. After turning on the high voltages, firstly, two oppositely charged fibrils flew to the end of the funnel with 1500 rpm rotation speed and a fiber membrane would be formed. Followed by switching on the winder collector of 13 rpm rotation speed, the membrane was dragged by a pre-suspended yarn connected with the winder collector. Then a rotodynamic fibrillar cone could be formed above the funnel. Simultaneously, fibers on the fibrillar cone were

pulled up in a spiral path. The whole electrospun yarn process was operated under the light of an infrared lamp (250 W) at about 45 °C and with about 10–15% of humidity.

The subsequent stretching processes were performed by a homemade roll-to-roll heat-stretching instrument consisting of three parts: a tubular furnace with one heat position zone (Heraeus, D6450 Hanau, Typ: RE 1.1, 400 mm in length, Germany), two rollers with electronic motors, and a laptop with "LV2016" controlling software for controlling the velocities of the motors. By adjusting the velocities of the two rollers by the LV2016 software, the yarn could be stretched continuously. The stretch ratio (SR) was calculated by the equation: SR = v_f/v_s , where v_f and v_s represent the velocities of fast roller and slow roller, respectively.

2.3. Fabrication of Uniform Short Fibers from Yarns

First, the yarn was wound into an aligned yarn bundle, which was immersed in ethanol and water for 5 min each, respectively, followed by freezing in liquid nitrogen and cutting into a fixed length (0.4 mm or 1.0 mm) by a homemade cutting tool (Figure S1, Supporting Information). The obtained short segments of yarn were dispersed in dioxane (0.5 mg mL⁻¹). A dispersion of short individual fibers of uniform length were obtained after sonification (sonorex super AK 514 BH, working at 35 kHz, HF powder: 215 W eff). This dispersion was freeze-dried for 48 h, which resulted in powder-like fibers. For comparison, 1 g of the stretched yarn was cut in cooled dioxane (1 L) by a mixer (Robot Coupe Blixer 4, Rudolf Lange GmbH & Co. KG) at 4000 rpm for several minutes until it became short fibers. After that, the polydisperse short fibers were obtained by freeze-drying for 48 h.

2.4. Fabrication of Sponges

In a typical experiment for the preparation of sponges with a density of about 7 mg cm⁻³, firstly, 3 mg of PU was dissolved

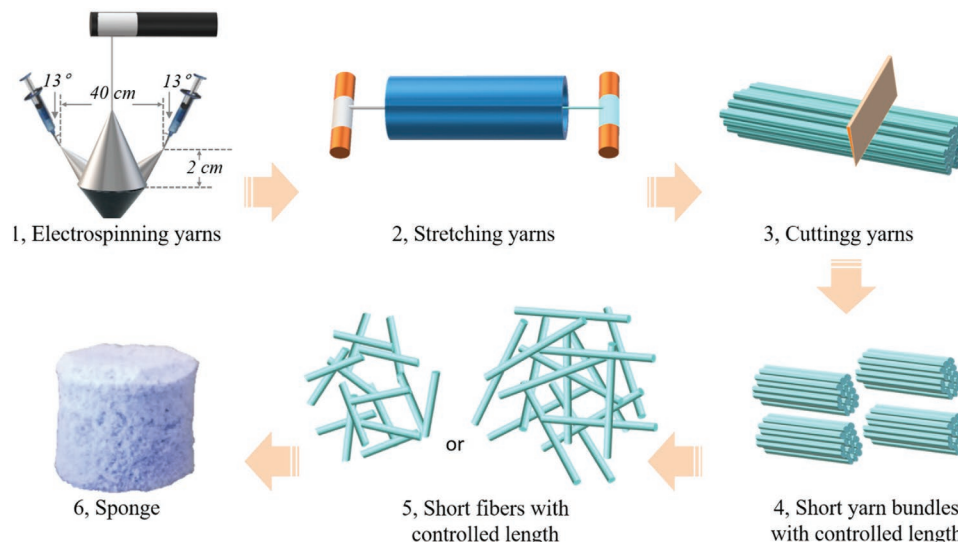


Figure 1. Schematic illustration of the fabrication process of sponge from short fibers with controlled length.



in 2.5 mL of dioxane, then 12 mg of short fibers were blended with the PU/dioxane solution. The obtained uniform dispersion was slowly cooled to -20°C , followed by freeze-drying for 48 h under 0.04 mbar. Finally, the sponges were annealed at 110°C for 2 h. The density of sponges was equal to the weight of sponge divided by the volume determination using radius and height of the cylindrical samples ($\pi r^2 h$). The sponges made of short fibers of controlled CV were obtained by mixing short fibers of 1.0 mm length and 0.4 mm length.

2.5. Characterization

Digital microscope (Smartzoom 5, Carl Zeiss AG) was used to observe the short fibers. The morphology of fibers, yarns, and sponges was studied by a Zeiss LEO 1530 (Gemini, Germany) scanning electron microscope (SEM). ImageJ software was used to measure the length of short fibers and the diameter of fibers and yarns based on an average of 100 fibers. According to a previous literature,^[39] the fiber alignment factors were calculated based on the equation: $d_{F\alpha} = (3\cos 2\theta - 1) / 2$, where $d_{F\alpha}$ is the fiber alignment factor and θ is the angle between the individual fibers and direction of the yarns. The given values were measured by ImageJ software based on an average of 100 fibers. Recycle loading-unloading compression tests were performed by zwickiLine Z0.5, BT1-FR0.5TN.D14, Zwick/Roell, Germany material tester, using a crosshead rate of 10 mm min^{-1} in air at room temperature. The load cell was a Zwick/Roell KAF TC with a nominal load of 20 N

3. Results and Discussion

The overall concept for the preparation of sponges with fibers of different lengths and fiber length distribution is shown in Figure 1. Following this concept, electrospun PAN yarns (diameter = $130 \pm 22 \mu\text{m}$) consisting of about 3000 unaligned individual fibers (diameter = $1.19 \pm 0.08 \mu\text{m}$) were obtained by continuous yarn electrospinning, followed by roll-to-roll heat stretching at 160°C and alignment of the fibers (diameter = $0.51 \pm 0.09 \mu\text{m}$, alignment factor = 99% at a stretch ratio of 6). The as-spun yarn showed random deposition of fibers. The alignment of the fibers in the yarn upon heat stretching was dependent upon the stretch ratio. The alignment factor for fibers changed from $\approx 48\%$ at stretch ratio 1 to about 99% at stretch ratio 6. The high degree of fiber alignment was important for getting short fibers with narrow length distribution on cutting.

Short fibers of two different lengths (416 ± 83 and $1034 \pm 156 \mu\text{m}$) were obtained by cryo-microcutting of the stretched yarns (Figure 2; Table S1, Supporting Information) in liquid nitrogen with a specially designed cutter (Figure S1, Supporting Information) and followed by ultrasonification in dioxane.

Notably, these short fibers exhibit tunable aspect ratio and narrow fiber length distribution, represented by the low CV values 15.1% and 20.0%, respectively (Figure 2; Figure S2 and Table S1, Supporting Information). Furthermore, the control experiment of making short fibers by mechanical cutting in a mixer, show fibers with uncontrollable length (average length

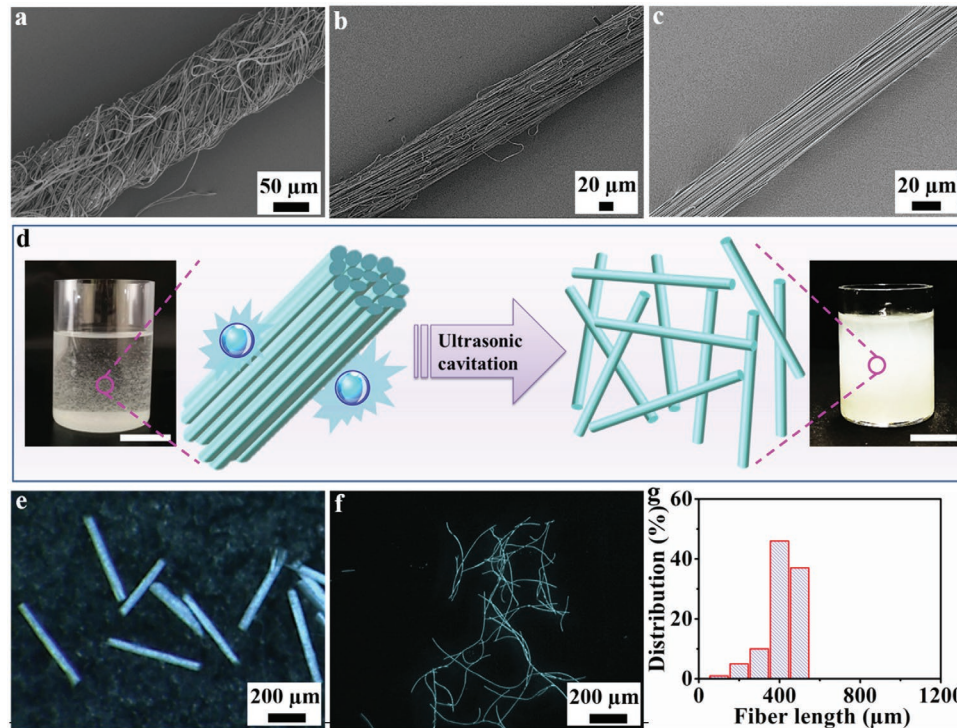


Figure 2. Microstructure and properties of yarns and fibers. SEM images of yarns with different stretch ratios: a) as-spun yarn, b) SR 3, and c) SR 6. d) Schematic representation of the ultrasonic cavitation process to produce individual fibers from short yarns. The inset digital pictures are dispersion of short yarns with 0.4 mm length (left) and corresponding dispersion of short fibers (right) in dioxane. The inset scale bar in the picture is 15 mm. Microscope pictures of: e) short yarns and f) fibers at 0.4 mm length. g) Fiber length distribution of short fibers made from cutter 0.4 mm.

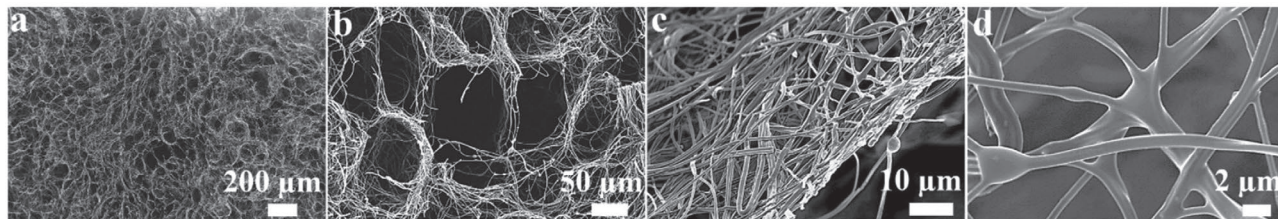


Figure 3. Cross-sectional SEM images of sponge made from short fibers of average length $416 \pm 83 \mu\text{m}$ in different magnifications. a) The whole cross-sectional image, b) the pore microstructure, c) the wall of pore, d) the glued individual fibers.

of $145 \pm 129 \mu\text{m}$) and broad length distribution with high CV of 89.0% (Figure S3 and Table S1, Supporting Information).

Short nanofibers (lengths 416 ± 83 and $1034 \pm 156 \mu\text{m}$) were dispersed in a dioxane solution of PU^[37] in different amounts for the preparation of the sponges. The addition of the particular PU was important due to its solubility in dioxane and its stickiness, which was required for binding of the fibers in the sponge. Different formulations made by dispersing short fibers and PU in dioxane were assembled into 3D porous sponges by freeze-drying process. Figure 3 shows the typical cross-sectional SEM images of a sponge (density of $\approx 7.0 \text{ mg cm}^{-3}$) made from short fibers of average length $416 \pm 83 \mu\text{m}$. The sponge showed dual pore-structure with small (pores between the fibers) and big pores (pore size of about $112 \pm 18.3 \mu\text{m}$ formed by sublimation of ice during freeze-drying). The sponge had open-cellular structure with highly interconnected pores through triangular or quadrangle junctions. Unique fibrous cell walls (big pore walls) consist of small pores between the fibers created by overlaying of the individual fibers in a regular, usual criss-cross pattern. Simultaneously, the PU as glue, assembled on the surface of fibers, which could induce further physical gluing and reinforce the mechanical properties of sponges.

In order to understand the role of the fiber length and its CV in the pore size, pore morphology, and compression strength of the sponges were compared (Figures 4 and 5; Table S2, Supporting Information). The cross-sectional SEM images of the sponges showed the typical disordered open-cellular structures. All sponges showed similar average visual pore sizes in the range of $112\text{--}118 \mu\text{m}$ as shown in the Figure 4. Thus, it

suggested that the length and length distribution of short fibers hardly affect the pore size of sponges. Compression test was done for 100 cycles of loading-unloading at maximum strain of 50% (Figure 5; Figure S4, Supporting Information). Sponges with low CV showed enhancement in stress by 32% and in modulus by 45%, in comparison to sponges with high CV. Moreover, the longer fibers (1.0 mm length) could endow the sponge with higher modulus than the shorter fibers (0.4 mm length) (Figure 5a,b). The energy loss coefficient became almost constant after first compression cycle showing the work done in compression and the energy loss remained the same in each cycle (Figure 5c). Similar behaviors were described for low density carbon-graphene monolith materials^[9] and for electrospun nanofiber aerogels.^[16]

4. Conclusions

Cryo-microcutting of multifibrillar electrospun fibrillar yarns results in short fibers of well-controlled length. Dispersion of short fibers with well-controlled fiber length distribution was obtained by mixing of short fibers of different lengths in dispersion. Sponges obtained from these dispersions by freeze-drying showed similar pore size and pore size distribution, but significantly higher compression strength and modulus for sponges with low CV. Sponges with low CV showed clearly higher compression strength and modulus. From this, we postulate that the mechanical properties of sponges could be tailored over a wide range by adjustment of fiber length which provides an additional

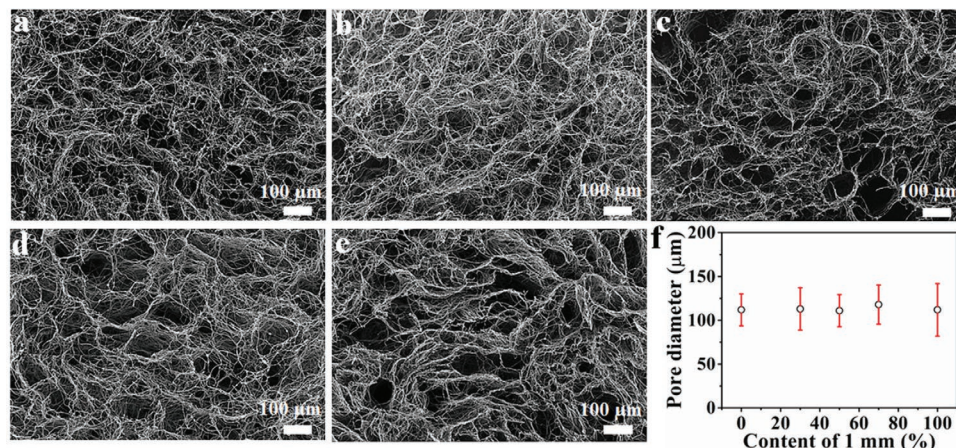


Figure 4. Microstructure of sponges. SEM cross-sectional images of sponges with different weight contents of 1 mm length short fibers: a) 0%, b) 30%, c) 50%, d) 70%, and e) 100%. f) Change of pore size in the sponge with different contents of 1 mm short fibers.

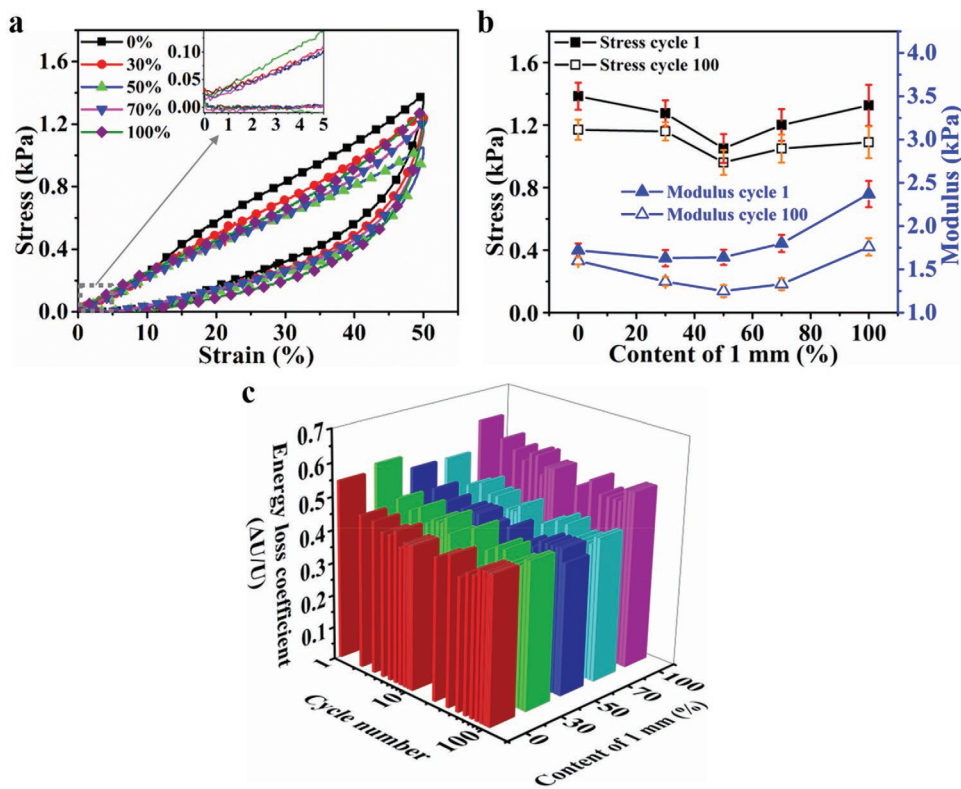


Figure 5. Microstructure and mechanical properties of sponges. a) Compression stress versus strain curves in compression test of sponges with different contents of 0.4 and 1.0 mm length short fibers. b) Changes of stress and modulus of sponges with different contents of 0.4 and 1 mm length short fibers during first and 100th cycle loading–unloading compression test. c) Changes of energy loss coefficient of the sponges with different contents of 0.4 and 1 mm length short fibers during 100 cycles compression test.

tool for tuning of sponge properties next to chemical treatments. Tailored mechanical properties will be of utmost importance for application of sponges, for example, in tissue engineering, sensors, electrodes, insulation materials, and textiles.

Received: September 19, 2019

Revised: November 3, 2019

Published online: January 13, 2020

Supporting Information

Supporting Information is available from the Wiley Online Library or from the author.

Acknowledgements

The authors acknowledge DFG (SFB 840) for financial support. The authors thank Peter Schmidt, Thomas Braun, and their co-workers in the workshops for help, design and building of the electrospun yarn setup, roll-to-roll stretching device, and cutting tool.

Conflict of Interest

The authors declare no conflict of interest.

Keywords

electrospinning, fiber lengths, mechanical properties, sponges, yarns

- [1] S. S. Kistler, *Nature* **1931**, *127*, 741.
- [2] A. Träger, A. Carlmark, L. Wågberg, *Macromol. Mater. Eng.* **2018**, *303*, 1700594.
- [3] S. Jiang, B. Uch, S. Agarwal, A. Greiner, *ACS Appl. Mater. Interfaces* **2017**, *9*, 32308.
- [4] J. Zhu, S. Jiang, H. Hou, S. Agarwal, A. Greiner, *Macromol. Mater. Eng.* **2018**, *303*, 1700615.
- [5] Y. Xiao, L. Li, S. Zhang, J. Feng, Y. Jiang, J. Feng, *Macromol. Mater. Eng.* **2019**, *304*, 1900137.
- [6] G. Hayase, K. Kanamori, G. Hasegawa, A. Maeno, H. Kaji, K. Nakanishi, *Angew. Chem., Int. Ed.* **2013**, *52*, 10788.
- [7] H. Sehaqui, Q. Zhou, L. A. Berglund, *Compos. Sci. Technol.* **2011**, *71*, 1593.
- [8] G. Duan, S. Jiang, V. Jérôme, J. H. Wendorff, A. Fathi, J. Uhm, V. Altstädt, M. Herling, J. Breu, R. Freitag, S. Agarwal, A. Greiner, *Adv. Funct. Mater.* **2015**, *25*, 2850.
- [9] H. Gao, Y. Zhu, L. Mao, F. Wang, X. Luo, Y. Liu, Y. Lu, Z. Pan, J. Ge, W. Shen, Y. Zheng, L. Xu, L. Wang, W. Xu, H. Wu, S. Yu, *Nat. Commun.* **2016**, *7*, 12920.
- [10] S. Jiang, S. Agarwal, A. Greiner, *Angew. Chem., Int. Ed.* **2017**, *56*, 15520.
- [11] Z. Qian, Z. Wang, N. Zhao, J. Xu, *Macromol. Rapid Commun.* **2018**, *39*, 1700724.



- [12] D. Lv, M. Zhu, Z. Jiang, S. Jiang, Q. Zhang, R. Xiong, C. Huang, *Macromol. Mater. Eng.* **2018**, *303*, 1800336.
- [13] S. Agarwal, S. Jiang, Y. Chen, *Macromol. Mater. Eng.* **2019**, *304*, 1800548.
- [14] S. S. Kistler, *J. Phys. Chem.* **1932**, *36*, 52.
- [15] H. Sun, Z. Xu, C. Gao, *Adv. Mater.* **2013**, *25*, 2554.
- [16] Y. Si, J. Yu, X. Tang, J. Ge, B. Ding, *Nat. Commun.* **2014**, *5*, 5802.
- [17] G. Duan, S. Jiang, T. Moss, S. Agarwal, A. Greiner, *Polym. Chem.* **2016**, *7*, 2759.
- [18] S. Jiang, N. Helffricht, G. Papastavrou, A. Greiner, S. Agarwal, *Macromol. Rapid Commun.* **2018**, *39*, 1700838.
- [19] T. Xu, Y. Ding, Z. Wang, Y. Zhao, W. Wu, H. Fong, Z. Zhu, *J. Mater. Chem. C* **2017**, *5*, 10288.
- [20] S. Jiang, S. Reich, B. Uch, P. Hu, S. Agarwal, A. Greiner, *ACS Appl. Mater. Interfaces* **2017**, *9*, 34286.
- [21] S. Jiang, V. Gruen, S. Rosenfeldt, A. S. Schenk, S. Agarwal, Z. Xu, A. Greiner, *Research* **2019**, *2019*, 1.
- [22] T. Xu, J. M. Miszuk, Y. Zhao, H. Sun, H. Fong, *Adv. Healthcare Mater.* **2015**, *4*, 2238.
- [23] M. Mader, V. Jerome, R. Freitag, S. Agarwal, A. Greiner, *Biomacromolecules* **2018**, *19*, 1663.
- [24] S. Jiang, G. Duan, J. Schöbel, S. Agarwal, A. Greiner, *Compos. Sci. Technol.* **2013**, *88*, 57.
- [25] W. Chen, J. Ma, L. Zhu, Y. Morsi, S. S. Al-Deyab, X. Mo, *Colloids Surf., B* **2016**, *142*, 165.
- [26] T. Xu, Z. Wang, Y. Ding, W. Xu, W. Wu, Z. Zhu, H. Fong, *Carbohydr. Polym.* **2018**, *179*, 164.
- [27] T. G. Kim, T. G. Park, *Macromol. Rapid Commun.* **2008**, *29*, 1231.
- [28] M. Sawawi, T. Y. Wang, D. R. Nisbet, G. P. Simon, *Polymer* **2013**, *54*, 4237.
- [29] I. W. Fathona, A. Yabuki, *J. Mater. Process. Technol.* **2013**, *213*, 1894.
- [30] C. F. Huang, C. Yoshikawa, K. Zhang, S. Hattori, T. Honda, E. Zawadzak, H. Kobayashi, *Adv. Mater. Res.* **2011**, *306-307*, 58.
- [31] I. W. Fathona, A. Yabuki, *J. Mater. Sci.* **2014**, *49*, 3519.
- [32] C. J. Luo, E. Stride, S. Stoyanov, E. Pelan, M. J. Edirisinghe, *J. Polym. Res.* **2011**, *18*, 2515.
- [33] S. Mahalingam, M. Edirisinghe, *Macromol. Rapid Commun.* **2013**, *34*, 1134.
- [34] A. Stoiljkovic, S. Agarwal, *Macromol. Mater. Eng.* **2008**, *293*, 895.
- [35] A. Omidinia-Anarkoli, S. Boesveld, U. Tuvshindorj, J. C. Rose, T. Haraszti, L. De Laporte, *Small* **2017**, *13*, 1702207.
- [36] K. J. Lee, J. Yoon, S. Rahmani, S. Hwang, S. Bhaskar, S. Mitragotri, J. Lahann, *Proc. Natl. Acad. Sci. USA* **2012**, *109*, 16057.
- [37] P. Hu, A. Greiner, S. Agarwal, *J. Polym. Sci., Part A-1: Polym. Chem.* **2019**, *57*, 752.
- [38] X. Liao, M. Dulle, J. Martins de Souza Silva, R. B. Wehrspohn, S. Agarwal, S. Förster, H. Hou, P. Smith, A. Greiner, *Science* **2019**, *366*, 1376.
- [39] R. Dersch, T. Liu, A. K. Schaper, A. Greiner, J. H. Wendorff, *J. Polym. Sci., Part A-1: Polym. Chem.* **2003**, *41*, 545.